Optical Damage Limits to Pulse Energy From Fibers

Arlee V. Smith, Binh T. Do, G. Ronald Hadley, and Roger L. Farrow

(Invited Paper)

***Abstract*—The irradiances or fluences encountered in pulsed fiber lasers and amplifiers are sometimes high enough to destroy the fiber. The ultimate limit is set by the intrinsic damage threshold irradiance of doped silica. Other nonlinear processes such as self-focusing and stimulated Brillouin scattering are also important. We present here the results of our measurements of the damage threshold, and of our analysis of how self-focusing and Brillouin scattering influence the power limit.**

***Index Terms*—Optical fiber amplifiers.**

I. Introduction

MANY applications of picosecond and nanosecond pulsed fiber amplifiers and lasers benefit from the highest possible pulse energies or powers, so it is worth exploring the ultimate power limits imposed by optical damage, self-focusing, and stimulated Brillouin scattering (SBS).

Maximizing the power/energy from pulsed fiber amplifiers forces designs in the direction of large mode areas and short fiber lengths. This maximizes the stored energy while minimizing the peak irradiance, and thus, the likelihood of optical damage. It also helps avoid the unwanted nonlinear processes of SBS and stimulated Raman scattering (SRS). In this paper, we provide a quantitative analysis of the limits imposed by self-focusing and optical damage in these fibers, and we discuss the role SBS might play in power limiting.

The literature contains several reports of multimegawatt power from passive picosecond fibers [1], and from nanosecond fiber amplifiers [2]–[6]. One paper [6] reports 4.5 MW peak powers, a power that approaches the expected self-focusing power for 1064 nm light in silica. Other papers report 27 mJ in 50 ns and 9.5 mJ in 4 ns from a 200-μm-diameter fiber [2]; 1 mJ, 1 ns pulses from a 41-μm-diameter core [3]; 2 MW in 7 ns pulses from a 35-μm-diameter core [4]; and 1.2 MW, 1.1 ns pulses from a 65-μm-diameter core [5]. Each of these cases imply fluences that match or exceed commonly cited damage fluences for silica [7]–[11].

Manuscript received September 11, 2008; revised October 28, 2008; accepted November 10, 2008. Current version published February 4, 2009. This work was supported by the United States Department of Energy (DOE) under Contract DE-AC04-94AL85000.

A. V. Smith is with AS-Photonics LLC, Albuquerque, NM 87112 USA (e-mail: arlee.smith@AS-Photonics.com).

B. T. Do is with the Ball Aerospace Corporation, Albuquerque, NM 87106 USA (e-mail: bto@ball.com).

G. R. Hadley is with Sandia National Laboratories, Albuquerque, NM 87123 USA (e-mail: grhadle@sandia.gov).

R. L. Farrow is with Sandia National Laboratories, Livermore, CA 94551 USA (e-mail: farrow@sandia.gov).

Color versions of one or more of the figures in this paper are available online at http://ieeexplore.ieee.org.

Digital Object Identifier 10.1109/JSTQE.2008.2010331

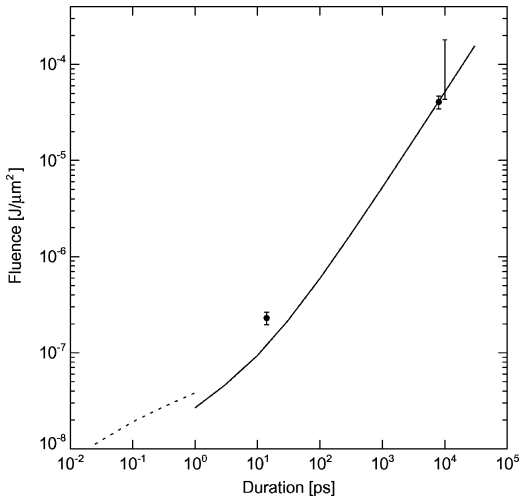

Fig. 1. Bulk damage threshold fluence of silica versus the pulse duration of 1064 nm light. The two data points are our measured values for 7 ns and 14 ps. The solid curve corresponds to the rate equation model given by (1), the dashed curve corresponds to the rate equation of Mero *et al.* [13] for 800 nm light, and the vertical bar corresponds to the dc breakdown threshold of Yasue *et al.* [14] scaled to the optical frequency of 1064 nm light.

II. Intrinsic Damage Threshold

Clearly, from the results just cited, silica damage thresholds for nanosecond pulses must be reexamined. In a recently completed study [12], we remeasured the intrinsic damage threshold of silica, and find it coincides with the highest value in all previous reports, and it is a factor of 50 higher than in the papers cited earlier. We can summarize our results by stating that the damage process for nanosecond and shorter pulses is an electron avalanche that is well modeled by the following rate equation governing the growth of free electrons

$$\frac{dn}{dt} = \beta I^k + \alpha I n - \frac{n}{\tau_r} \tag{1}$$

where n is the free electron density, β is the multiphoton ionization cross section, I is the irradiance, k is the number of photons required to ionize the material, α is the electron avalanche coefficient, and τ_r is the electron recombination lifetime. Approximate values for 1064 nm light are $\beta = 2 \times 10^{-19}$ μm^{13}/W^8·s, $\alpha = 8.3 \times 10^8$ μm^2/J, and $\tau_r = 250$ fs. Damage is assumed if n exceeds 2×10^8 μm^{-3} at any time during the pulse. At this electron density, the plasma frequency nearly equals the optical frequency, so the incoming light is absorbed in less than 1 μm. The deposited energy is sufficient to melt or fracture the glass. Our measured and modeled thresholds for different pulse durations are plotted in Fig. 1. Corroborative evidence from femtosecond–picosecond studies with 800 nm

pulses [13], and from the dc breakdown threshold [14] are also included in the figure.

For pulses much longer than τ_r ($\tau > 50$ ps), damage occurs at a nearly constant irradiance of 4.75 kW/μm^2. This makes the threshold fluence linear in τ for pulses longer than 50 ps. For shorter pulses, the avalanche evolves more slowly than the pulse envelope, so the threshold fluence lies above the line extrapolated from long pulses.

Our damage threshold measurements are made in pure silica. We do not know the precise influence of Yb^{3+} or other dopants on the damage threshold, but preliminary evidence from studies in our laboratory indicate that Yb doping does not noticeably lower it.

III. Self-Focusing in Fibers

To determine whether the peak fluence exceeds the damage threshold we must know how self-focusing affects the mode profile. At high irradiances, the refractive index is altered by the addition of a nonlinear contribution

$$n = n_\circ + n_2 I \tag{2}$$

where $n_\circ$ is the refractive index at low irradiance, I is the irradiance, and n_2 is the nonlinear refractive index, which is usually positive, leading to self-focusing at high powers. In this paper, we will assume that n_2 is the same in the core and cladding. If it is not, some details of our analysis must be changed, but the critical self-focusing power will be unchanged.

We begin by discussing self-focusing of CW beams. Chiao *et al.* [15] showed that for a certain critical power, self-focusing and diffraction can exactly cancel one another in a bulk medium if the circularly symmetric radial profile of the beam is that of the Townes soliton. This profile differs slightly from a lowest order Gaussian [15], [16]. A beam perfectly matching this profile would propagate without change. However, it is unstable, so in practice small imperfections grow, destroying the soliton. The critical power is given by

$$\mathcal{P}_{\rm SF} = \frac{0.148\lambda^2}{n_\circ n_2}. \tag{3}$$

The size of the beam can be freely scaled so it has no defined size [17] but instead is defined by a definite shape and power. For higher powers, self-focusing overcomes diffraction, causing the beam to focus to a tiny spot. For lower powers, diffraction dominates and the beam diverges. Townes solitons are not directly relevant to waveguides, except that we will see the critical self-focusing power to be exactly the same in fibers as in the soliton.

Beams that are focused on the input face of a bulk sample, and that have a radial irradiance profile different from the Townes soliton, require slightly higher power to self-focus because some of the power is shed from the core of the beam in the course of propagating to the self-focusing point. For example, a lowest order gaussian beam requires a power approximately 2% higher than $\mathcal{P}_{\rm SF}$ to self-focus. However, a gaussian beam focused deep in a bulk sample, rather than at the input face, requires exactly $\mathcal{P}_{\rm SF}$ to self-focus. Further, $\mathcal{P}_{\rm SF}$ completely characterizes the incipient self-focusing behavior of a deep focus gaussian beam [12], [17]. For powers lower than $\mathcal{P}_{\rm SF}$, the on-axis irradiance is enhanced by self-focusing according to the expression

$$\frac{I}{I_\circ} = \frac{1}{1 - \mathcal{P}/\mathcal{P}_{\rm SF}} \tag{4}$$

where $I_\circ$ is the peak on axis irradiance in the absence of self-focusing. For powers exceeding $\mathcal{P}_{\rm SF}$, self-focusing develops fully, leading to a tiny focal spot and inevitable optical damage.

The question of interest in this paper is how self-focusing behaves in a fiber. Is the critical power for the lowest order mode equal to $\mathcal{P}_{\rm SF}$? Is the on-axis irradiance enhancement still characterized by (4)? Fibich and Gaeta [16] and Fibich and Merle [18] showed the critical power in hollow waveguides is indeed exactly $\mathcal{P}_{\rm SF}$. They used numerical propagation of continuous-wave (CW) beams, with the mode amplitude forced to zero at the core walls, to reach their conclusion. We have applied both beam propagation modeling and fixed power calculations of the lowest order mode to deduce that the same conclusion holds for unbent fibers with an elevated core index in the cases of step-index and parabolic-index profiles. We have also computed the approximate curves for the on-axis enhancement $I/I_\circ$ for these fibers, and find that the enhancement due to self-focusing is more abrupt in fibers than in the bulk as the power approaches the critical power $\mathcal{P}_{\rm SF}$.

Our propagation model starts by injecting the low-power, lowest order eigenmode into the fiber and gradually amplifying it as it propagates. The on-axis irradiance and mode diameter are computed for each power level. The amplification is gradual enough that mode mixing is avoided, so the propagating mode is always the lowest order mode for the corresponding local power. We also computed the mode profile by iteratively adding the nonlinear index term to $n(r)$. We used both finite-element calculations and a mode expansion method. The latter follows the Bessel function expansion presented by Marcuse [19]. We separate the field into a radial and azimuthal parts in the form

$$E(r,\phi) = E(r)\cos(\nu\phi). \tag{5}$$

The radial part of the field must satisfy

$$\frac{d^2E(r)}{dr^2} + \frac{1}{r}\frac{dE(r)}{dr} + \left[n^2(r)\frac{\omega^2}{c^2} - \beta^2 - \frac{\nu^2}{r^2}\right]E(r) = 0. \tag{6}$$

Expanding $E(r)$ in terms of Bessel functions

$$E(r) = \sum_{\mu=1}^{N} c_\mu J_\nu(\kappa_\mu r) \tag{7}$$

and confining the functions to an area with radius R, the κ_μ's are related to the roots of the Bessel function w_μ by

$$\kappa_\mu = \frac{w_\mu}{R}. \tag{8}$$

Choosing a value for the angular frequency ν, the values for β and c_μ are the eigenvalues and eigenvectors of the matrix

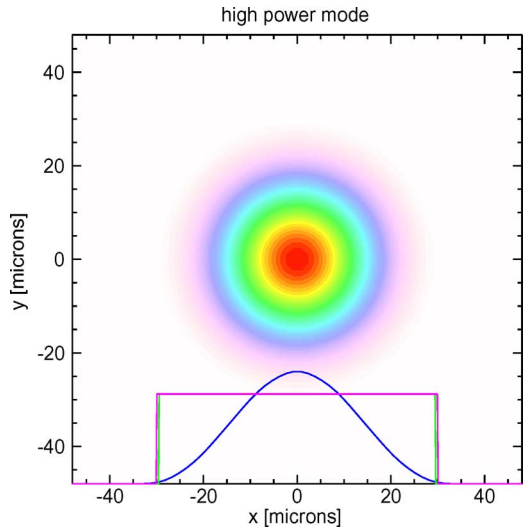

Fig. 2. Mode profile for a fiber with core radius of 30 μm, NA = 0.06, λ = 1064 nm, $n_2 = 2.7 \times 10^{-20}$ m^2/W, and power of 0.1 MW ($\mathcal{P}/\mathcal{P}_{\rm SF} = 0.023$).

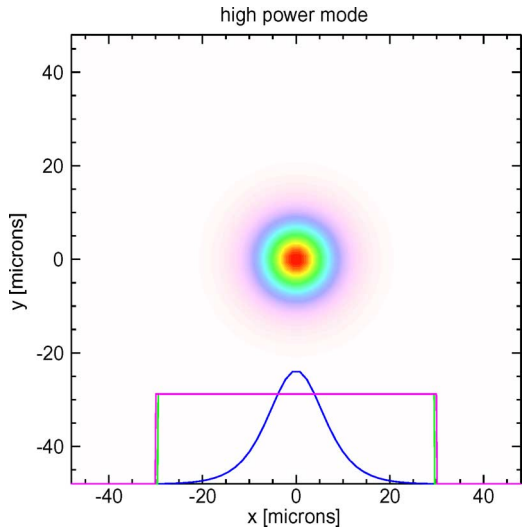

Fig. 3. Mode profile under identical conditions to Fig. 2 except at a power of 4.0 MW ($\mathcal{P}/\mathcal{P}_{\rm SF} = 0.93$).

A whose elements are

$$A_{\mu'\mu} = \frac{2}{R^2 J_{\nu+1}^2(\kappa_{\mu'} R)} \int_0^R \left[(n_{\rm core}^2(r) - n_{\rm clad}^2) \times r J_\nu(\kappa_{\mu'} r) J_\nu(\kappa_\mu r) dr\right] - \frac{c^2 \kappa_\mu^2}{\omega^2} \delta_{\mu'\mu}. \quad (9)$$

The matrix A can be constructed for any circularly symmetric core refractive index profile $n(r)$ and numerically diagonalized to find the propagation constant β and the eigenvectors c_μ. To compute the high-power fundamental mode, the nonlinear contribution $n_{\rm nl}(r) = n_2 I(r)$ is added to $n_{\rm core}(r)$ and the mode is recomputed. Here, $I(r)$ is the irradiance of the last previously computed fundamental mode. This process is iterated until convergence is achieved.

The modes computed using these three independent methods are indistinguishable. As an illustration of modal constriction by self-focusing, Figs. 2 and 3 compare mode profiles in the same step-index fiber at different powers. At high power, the mode is confined to the center of the core and barely samples the cladding, so it is not surprising that the critical self-focusing power is the same as in the bulk.

We find that for parabolic index profiles with low power modal areas of 1200 and 570 μm^2, the on-axis enhancement is reasonably well approximated by

$$\frac{I}{I_\circ} = \frac{1}{(1 - \mathcal{P}/\mathcal{P}_{\rm SF})^{0.63}}. \quad (10)$$

There is only a small difference in the enhancement between fibers with the 570 and 1200 μm^2 modal areas. Other papers give somewhat different results. For example, Romanova *et al.* [20] say the exponent is 0.5 rather than 0.63 in parabolic index fiber. However, they assume the lowest order mode has a gaussian profile, which is a poor assumption for large-mode-area fibers.

For step-index profiles with numerical aperture (NA) = 0.06 and core radii ranging from 10 to 60 μm, the on-axis irradiance enhancement is approximated by

$$\frac{I}{I_\circ} = \frac{1}{(1 - \mathcal{P}/\mathcal{P}_{\rm SF})^{0.46}} \quad (11)$$

again with only small differences for the different core sizes. Fig. 4 compares the on-axis irradiance enhancement for step-index and parabolic-index fibers with the enhancement in bulk samples with deep focusing. Clearly, the onset of self-focusing is more abrupt in the waveguides than in the bulk. We did not study step-index fibers with other NA values, but 0.06 is typical of large-mode-area fibers. We have described a self-focusing calculation applicable only to straight fibers, but we find using the finite element and propagation methods that there is no substantial difference between bent and straight fibers [21].

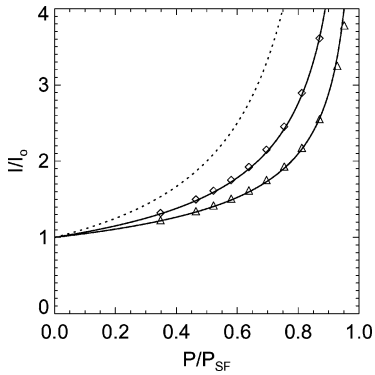

Fig. 4. On-axis irradiance enhancements due to self-focusing computed for a straight fiber with a step index and NA = 0.06 (triangles), and a parabolic-index profile (diamonds), along with the approximate scaling curves given by (11) for the step index and (10) for the parabolic index (solid curves). For reference, the dashed curve is the self-focusing enhancement for a bulk sample given by (4).

In Fig. 5 we show the on-axis irradiance versus power for step-index fibers of different core sizes, all with NA = 0.06. Plotting the powers at the intersection of each curve with our measured damage threshold of 4.75 kW/μm^2 gives the damage-limited curve of Fig. 6. For cores with radius smaller

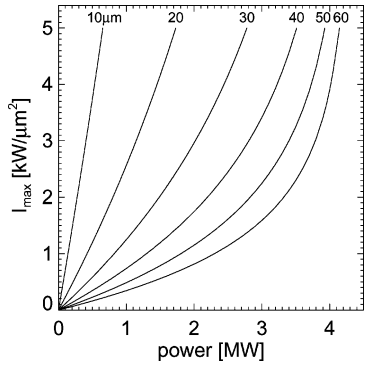

Fig. 5. On-axis irradiance versus power for straight, step index fibers with core radii 10-60 μm, NA $= 0.06$, $n_{\rm core} = 1.45$, $\lambda = 1064$ nm, $n_2 = 2.7 \times 10^{-20}$ m^2/W. The silica damage threshold is approximately 4.75 kW/μm^2.

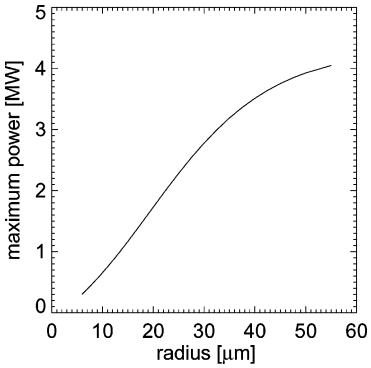

Fig. 6. Damage-limited power versus core radius for straight step-index fibers with numerical aperture of 0.06, $n_{\rm core} = 1.45$, $n_2 = 2.7 \times 10^{-20}$ m^2/W.

than 30 μm damage occurs at power levels well below $\mathcal{P}_{\rm SF}$ so the maximum is not much affected by self-focusing. For larger cores, the influence of self-focusing is apparent, and there is relatively little benefit from increasing the core size.

The dominant contribution to n_2 in silica comes from the Kerr effect [22]. It is instantaneous on the ns-ps time scale, and for linearly polarized light, it contributes 2.2×10^{-20} m^2/W (corresponding to $\mathcal{P}_{\rm SF} = 5.2$ MW). For circularly polarized light, the value is two-third as large ($\mathcal{P}_{\rm SF} = 7.8$ MW). Electrostriction also contributes to n_2, but it takes time to pull material into the high irradiance region. The electrostrictive contribution is polarization independent and contributes a maximum of 0.5×10^{-20} m^2/W to n_2. For pulses longer than approximately 5 ns, electrostriction can contribute fully in a large-mode-area fiber [23], reducing the self-focusing power to 4.25 MW for linearly polarized light or 5.84 MW for circularly polarized light. For pulses shorter than 100 ps, electrostriction is negligible.

It is not known whether n_2 is affected by Yb^{3+} doping in gain fiber, but there is a known time-dependent Kramers–Kronig contribution to the refractive index that is due to the changing population inversion during amplification of a pulse [24]. This causes a slight defocusing of the trailing edge of the pulse. We are ignoring this effect.

A. Mode Stability at High Power

One idea for exceeding the power limit $\mathcal{P}_{\rm SF}$ is to use higher order modes. For example, the LP_{11} mode contains two lobes. If the power in each lobe can approach $\mathcal{P}_{\rm SF}$, we could double the power limit. Modes with N lobes could transmit powers approaching $N\mathcal{P}_{\rm SF}$. Computing the mode profiles using the iterative mode calculation method described earlier indicates that this approach is promising. However, it does not address the issue of mode stability. That can be studied using the beam propagation models. We find that the two-lobed mode is unstable. Slight upsets to the balance in power in the two lobes tend to grow, with the power oscillating between the modes, until eventually all of the power is in the single lobe of the lowest order mode where it remains. This instability of higher order modes has been noted in other reports. For instance, Romanova *et al.* [20] found that the LP_{02} mode of a double-moded fiber decays into the lowest radial mode in presence of Kerr nonlinearity. Further, they stated that the decay occurs over a shorter distance for higher powers. We add the observation that vortex modes are likewise unstable against decay to the lowest order mode. They first form a number of lobes with the number depending on the vortex charge [25], then these lobes coalesce into the single lobe of the lowest order mode. Evidently, only the lowest order mode is stable at high power, so one cannot exceed $\mathcal{P}_{\rm SF}$ using such mode engineering. Konorov *et al.* [26] experimentally found evidence of a decay of high-order modes into the lowest order mode in a gas-filled, hollow core, photonic crystal fiber.

IV. SBS Contribution to Damage

Anecdotal evidence suggests that fiber damage often coincides with the SBS threshold. SBS generates a Stokes wave redshifted by 15 GHz (for 1064 nm light) and travelling in the opposite direction to the pump wave. The two waves form an interference pattern that moves at the acoustic velocity. At each location in the fiber, the irradiance is modulated at 15 GHz, but this is sufficiently slow for the electron avalanche to respond to the peak irradiance. If the peak irradiance exceeds the damage threshold of approximately 5 kW/μm^2, it will cause damage.

In addition, the Stokes wave can assist in the self-focusing process via cross-phase modulation, which is twice as strong as self-phase modulation. The Stokes wave can also sweep energy out of the pump pulse leading to shorter, more intense pulses with peak irradiance well in excess of the peak irradiance of the pump. Which of these effects contributes most to damage may vary case by case, but it is clear that SBS can reduce the maximum achievable pump power by a factor of two or more. For pulses shorter than 1 ns, self-phase modulation caused by n_2 will tend to suppress SBS in typical large-mode-area fiber applications. For longer pulses, maximizing the power may require other means of SBS suppression. A number of methods can be used, including frequency modulation of the input pulse, or varying the acoustic velocity along or across the fiber using temperature, composition, or strain gradients.

V. Summary

The intrinsic damage threshold of silica is now well known for femtosecond to nanosecond pulses [12]. The damage fluences are shown in Fig. 1. The influence of Yb^{3+} doping on the damage threshold is not precisely known but preliminary evidence from our laboratory indicates it does not reduce it significantly. To use this threshold to infer maximum pulse power, we must also know the mode profile in the presence of self-focusing. From our calculations, self-focusing plays a major role only if the modal area at low power exceeds 500 μm^2, or in straight fiber, the core radius exceeds 20 μm. For smaller modal areas, the damage threshold is reached at powers well below the self-focusing power $\mathcal{P}_{SF}$. If SBS is above threshold it can reduce the threshold damage power by a factor of two or more. Tightly bending a large-mode-area fiber tends to compress the lowest order mode quite strongly, reducing the effective modal area or the effective core diameter accordingly. Bending is commonly used to filter out higher order modes, but it also tends to limit the output power, both by encouraging SBS and by increasing the peak irradiance. Finally, damage develops on a picosecond time scale, so spectrally broadened pulses, such as those from a multi longitudinal-mode laser, with large amplitude modulation will have substantially reduced transmissible fluence compared with spectrally narrow pulses.

Acknowledgment

Sandia is a multiprogram laboratory operated by Sandia Corporation, a Lockheed Martin Company, for the United States Department of Energy.

References

[1] L. A. G. Jahn, J. J. Kasinski, and R. J. D. Miller, "High-energy handling capabilities of optical fibers: Application to pulse compression and direct generation of megawatt picosecond pulses," *Appl. Phys. A, Solids Surf.*, vol. 43, pp. 41–46, 1987.

[2] M.-Y. Cheng, Y.-C. Chang, A. Galvanauskas, P. Mamidipudi, R. Changkakoti, and P. Gatchell, "High-energy and high-peak-power nanosecond pulse generation with beam quality control in 200-μm core highly multimode Yb-doped fiber amplifiers," *Opt. Lett.*, vol. 30, pp. 358–360, 2005.

[3] C. D. Brooks and F. D. Teodoro, "High peak power operation and harmonic generation of a single-polarization, Yb-doped photonic crystal fiber amplifier," *Opt. Commun.*, vol. 280, pp. 424–430, 2007.

[4] O. Schmidt, J. Rothardt, F. Roser, S. Linke, T. Schreiber, K. Rademacher, J. Limpert, S. Ermeneux, P. Yvernault, F. Salin, and A. Tunnermann, "Millijoule pulse energy Q-switched short-length fiber laser," *Opt. Lett.*, vol. 32, pp. 1551–1553, 2007.

[5] S. Desmoulins and F. D. Teodoro, "High-gain Er-doped fiber amplifier generating eye-safe MW peak-power, mJ-energy pulses," *Opt. Express*, vol. 16, pp. 2431–2437, 2008.

[6] F. D. Teodoro and C. D. Brooks, "Multistage Yb-doped fiber amplifier generating megawatt peak-power, subnanosecond pulses," *Opt. Lett.*, vol. 30, pp. 3299–3301, 2005.

[7] J. H. Campbell, F. Rainer, M. Kozlowski, C. R. Wolfe, I. Thomas, and F. Milanovich, "Damage resistant optics for a mega-joule solid-state laser," *Proc. SPIE*, vol. 1441, pp. 444–456, 1991.

[8] N. Kuzuu, K. Yoshida, H. Yoshida, T. Kamimura, and N. Kamisugi, "Laser-induced bulk damage in various types of vitreous silica at 1064, 532, 355, and 266 nm: Evidence of different damage mechanisms between 266 nm and longer wavelengths," *Appl. Opt.*, vol. 38, pp. 2510–2515, 1999.

[9] D. Du, X. Liu, G. Korn, J. Squier, and G. Mourou, "Laser-induced breakdown by impact ionization in SiO_2 with pulse widths from 7 ns to 150 fs," *Appl. Phys. Lett.*, vol. 64, pp. 3071–3073, 1994.

[10] B. C. Stuart, M. D. Feit, S. Herman, A. M. Rubenchick, B. W. Shore, and M. D. Perry, "Laser-induced damage in dielectrics with nanosecond to subpicosecond pulses," *Phys. Rev. Lett.*, vol. 74, pp. 2248–2251, 1995.

[11] A. C. Tien, S. Backus, H. Kapteyn, M. M. Murnane, and G. Mourou, "Short-pulse laser damage in transparent materials as a function of pulse duration," *Phys. Rev. Lett.*, vol. 82, pp. 3883–3886, 1999.

[12] A. V. Smith and B. T. Do, "Bulk and surface laser damage of silica by picosecond and nanosecond pulses at 1064 nm," *Appl. Opt.*, vol. 47, pp. 4812–4832, 2008.

[13] M. Mero, J. Liu, W. Rudolph, D. Ristau, and K. Starke, "Scaling laws of femtosecond laser induced breakdown in oxide films," *Phys. Rev. B, Condens. Matter*, vol. 71, pp. 115 109-1–115 109-7, 2005.

[14] T. Yasue, Y. Yoshida, H. Koyama, T. Kato, and T. Nishioka, "Dielectric breakdown of silicon dioxide studied by scanning probe microscopy," *J. Vac. Sci. Technol. B, Microelectron Process. Phenom.*, vol. 15, pp. 1884–1888, 1997.

[15] R. Y. Chiao, E. Garmire, and C. H. Townes, "Self-trapping of optical beams," *Phys. Rev. Lett.*, vol. 13, pp. 479–482, 1964.

[16] G. Fibich and A. L. Gaeta, "Critical power for self-focusing in bulk media and in hollow waveguides," *Opt. Lett.*, vol. 25, pp. 335–337, 2000.

[17] J. H. Marburger, "Self-focusing: Theory," *Prog. Quantum Electron.*, vol. 4, pp. 35–110, 1975.

[18] G. Fibich and F. Merle, "Self-focusing on bounded domains," *Physica D*, vol. 155, pp. 132–158, 2001.

[19] D. Marcuse, *Theory of Dielectric Optical Waveguides*. New York: Academic, 1974.

[20] E. A. Romanova, L. A. Melnikov, and E. V. Bekker, "Light guiding in optical fibers with Kerr-like nonlinearity," *Microw. Opt. Technol. Lett.*, vol. 30, pp. 212–216, 2001.

[21] R. L. Farrow, D. A. V. Kliner, G. R. Hadley, and A. V. Smith, "Peak-power limits on fiber amplifiers imposed by self-focusing," *Opt. Lett.*, vol. 31, pp. 3423–3425, 2006.

[22] R. Adair, L. L. Chase, and S. A. Payne, "Nonlinear refractive index of optical crystals," *Phys. Rev. B, Condens. Matter*, vol. 39, pp. 3337–3350, 1989.

[23] E. L. Kerr, "Transient and steady-state electrostrictive laser beam trapping," *IEEE J. Quantum Electron.*, vol. QE-6, no. 10, pp. 616–621, Oct. 1970.

[24] J. W. Arkwright, P. Elango, G. R. Atkins, T. Whitbread, and M. J. F. Digonnet, "Experimental and theoretical analysis of the resonant nonlinearity in ytterbium-doped fiber," *J. Lightw. Technol.*, vol. 16, no. 5, pp. 798–806, 1998.

[25] L. T. Vuong, T. D. Grow, A. Ishaaya, A. L. Gaeta, G. W. 't Hooft, E. R. Eliel, and G. Fibich, "Collapse of optical vortices," *Phys. Rev. Lett.*, vol. 96, pp. 133 901-1–133 901-4, 2006.

[26] S. O. Konorov, A. M. Zheltikov, P. Zhou, A. P. Tarasevitch, and D. von der Linde, "Self-channeling of subgigawatt femtosecond laser pulses in a ground-state waveguide induced in the hollow core of a photonic crystal fiber," *Opt. Lett.*, vol. 29, pp. 1521–1523, 2004.

Arlee V. Smith received the B.S. degree in physics from Alma College, Alma, MI, and the Ph.D. degree in physics from the University of Michigan, Ann Arbor.

From 1979 to 1980, he was a Postdoctoral Fellow at the Joint Institute for Laboratory Astrophysics (JILA) before joining Sandia National Laboratories, Albuquerque, NM, where he had a 28-year stint. During his stay at Sandia, he was engaged in atomic/molecular spectroscopy and nonlinear optics, laser physics, and crystal nonlinear optics. He recently retired from Sandia and formed AS-Photonics LLC, an optics consulting company located at Albuquerque. Dr. Smith is a Fellow of the Optical Society of America.

Binh T. Do received the Ph.D. degree in physics from Purdue University, West Lafayette, IN, in 2003.

He was with Sandia National Laboratories, Albuquerque, NM, as a Postdoctoral Fellow. He is currently with the Ball Aerospace Corporation, Albuquerque, where he is engaged in research on laser-induced optical damage.

G. Ronald Hadley received the B.A. degree in physics from Wichita State University, Wichita, KS, in 1968, and the Ph.D. degree in physics from Iowa State University, Ames, in 1972.

Since 1972, he has been with Sandia National Laboratories, Albuquerque, NM. He is the author or coauthor of more than 60 publications, most of them involving computer simulations, including current flow in high-voltage vacuum diodes, two-phase flow of liquids through porous media, and the operation of solid state and gas lasers. Since 1985, his research has centered on photonics, and most of his publications have dealt with the numerical modeling of diode lasers or diffractive waveguide optics components. His most important recent contributions include new higher order accurate finite-difference algorithms for beam propagation, waveguide eigenmode computation, the modeling of reflective optical structures, and the simulation of vertical-cavity surface-emitting lasers.

Roger L. Farrow received the B.A. degrees in physics and mathematics from the University of the South, Sewanee, TN, in 1974, and the Ph.D. degree in engineering and applied science from Yale University, New Haven, CT, in 1979.

Since 1979, he has been a Member of Technical Staff at Sandia National Laboratories, Livermore, CA, where he has been engaged in research in the areas of experimental linear and nonlinear laser spectroscopy for combustion measurements, high-intensity light–matter interactions, and fiber laser and detector development for remote sensing and chemical analysis.